Estuarine, Coastal and Shelf Science 79 (2008) 661–670

Contents lists available at ScienceDirect

Estuarine, Coastal and Shelf Science

journal homepage: www.elsevier.com/locate/ecss

Turbulence characteristics of a small subtropical estuary during and after some moderate rainfall

Mark Trevethan [a], Hubert Chanson [a,*], Richard Brown [b]

[a] Division of Civil Engineering, The University of Queensland, Brisbane, Qld 4072, Australia
[b] Engineering Systems, Queensland University of Technology, Brisbane, Qld 4000, Australia

ARTICLE INFO

Article history:
Received 27 March 2008
Accepted 11 June 2008
Available online 18 June 2008

Keywords:
turbulence
small subtropical estuary
covariances
triple correlations
field measurements
acoustic Doppler velocimetry
rainfall runoff

ABSTRACT

In natural estuaries, scalar diffusion and dispersion are driven by turbulence. In the present study, detailed turbulence measurements were conducted in a small subtropical estuary with semi-diurnal tides under neap tide conditions. Three acoustic Doppler velocimeters were installed mid-estuary at fixed locations close together. The units were sampled simultaneously and continuously at relatively high frequency for 50 h. The results illustrated the influence of tidal forcing in the small estuary, although low-frequency longitudinal velocity oscillations were observed and believed to be induced by external resonance. The boundary shear stress data implied that the turbulent shear in the lower flow region was one order of magnitude larger than the boundary shear itself. The observation differed from turbulence data in a laboratory channel, but a key feature of natural estuary flow was the significant three-dimensional effects associated with strong secondary currents including transverse shear events. The velocity covariances and triple correlations, as well as the backscatter intensity and covariances, were calculated for the entire field study. The covariances of the longitudinal velocity component showed some tidal trend, while the covariances of the transverse horizontal velocity component exhibited trends that reflected changes in secondary current patterns between ebb and flood tides. The triple correlation data tended to show some differences between ebb and flood tides. The acoustic backscatter intensity data were characterised by large fluctuations during the entire study, with dimensionless fluctuation intensity $I'_b/\overline{I_b}$ between 0.46 and 0.54. An unusual feature of the field study was some moderate rainfall prior to and during the first part of the sampling period. Visual observations showed some surface scars and marked channels, while some mini transient fronts were observed.

1. Introduction

In natural estuaries, contaminant transport and scalar dispersion are driven by turbulence mixing. Relatively little systematic research has been conducted on the turbulence characteristics of small estuaries. Past measurements were conducted typically for short periods or in bursts: e.g. Bowden and Ferguson (1980); Shiono and West (1987); Kawanisi and Yokosi (1994); Stacey et al. (1999); van de Ham et al. (2001); Nikora et al. (2002); Kawanisi (2004); Voulgaris and Meyers (2004); Ralston and Stacey (2005). Most data lacked spatial and temporal resolution to gain some insight into the characteristics of fine scale turbulence.

Herein detailed turbulence field measurements were conducted continuously at relatively high frequency for 2 days in a small subtropical estuary with semi-diurnal tides. Three acoustic Doppler velocimeters were sampled simultaneously at fixed locations in the mid-estuarine zone. The results provided a unique characterisation of the estuarine turbulence. An unusual feature of the study was some moderate rainfall for the first 24 h.

2. Study site and instrumentation

2.1. Field investigation and sampling site

The field study was conducted in the small subtropical estuary of Eprapah Creek (Redlands, Qld, Australia) in eastern Australia under neap tide conditions (Fig. 1). The estuarine zone is 3.8 km long, about 1–2 m deep mid-stream, and about 20–30 m wide. This is a relatively small, narrow, elongated and meandering channel with a cross-section which deepens and widens towards the mouth, and surrounded by extensive mudflats. For example, the hydraulic diameter at mean sea level varied from 4.9, 3.5 and 3.6 m, respectively, at 1, 2.1 and 3.3 km from the river mouth, corresponding to Sites 1, 2B and 3 in Fig. 1. The catchment area is about 40 km^2 and the creek flows directly into Moreton Bay off the Pacific Ocean. The estuary is a drowned river valley type with a wet and dry tropical/subtropical hydrology that

* Corresponding author.
E-mail address: h.chanson@uq.edu.au (H. Chanson).

0272-7714/$ – see front matter © 2008 Elsevier Ltd. All rights reserved.
doi:10.1016/j.ecss.2008.06.006

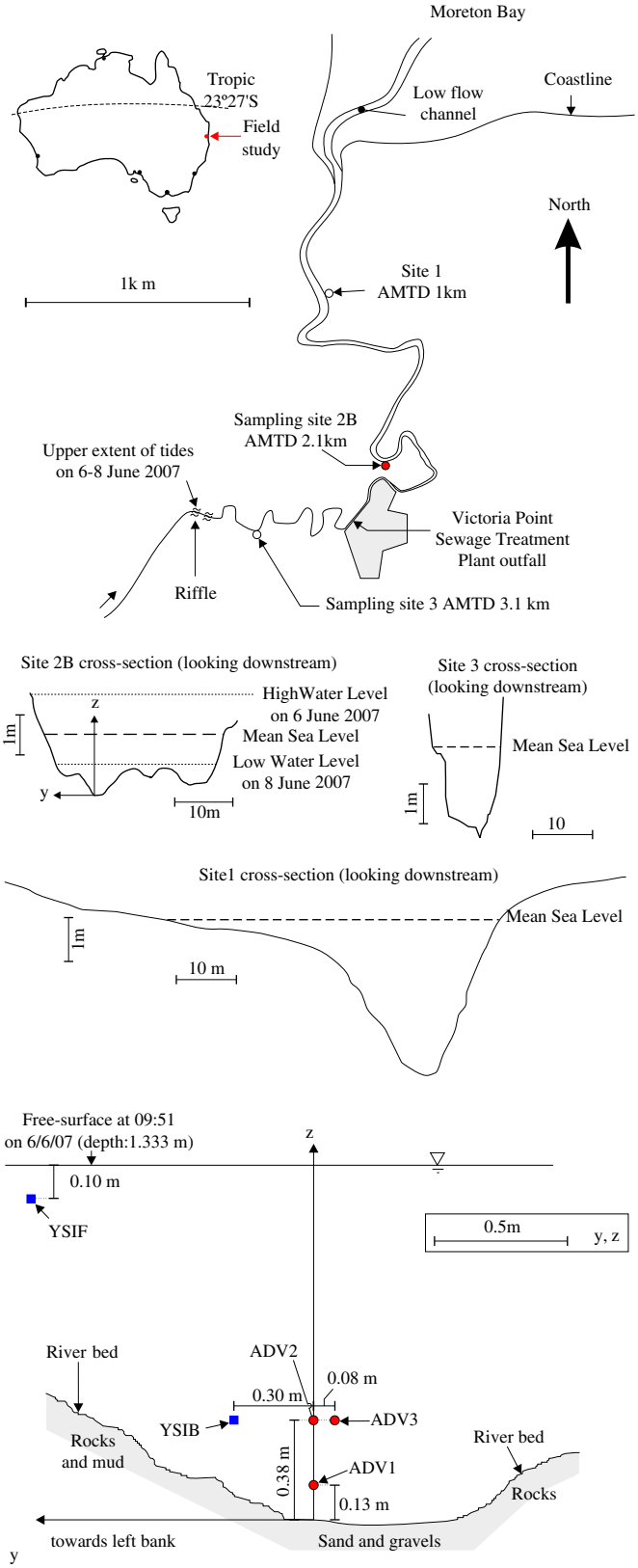

Fig. 1. Estuarine zone of Eprapah Creek, Australia. (A) Dimensioned map based upon an aerial photograph. (B) Surveyed cross-sections (looking downstream). (C) Dimensioned sketch of the ADV and YSI probe sampling volumes at Site 2B with the free-surface elevation at 09:51 on 6 June 2007, looking downstream.

accounts for nearly one third of all estuaries in Australia (Digby et al., 1999). Although the tides are semi-diurnal, the tidal cycles have slightly different periods and amplitudes indicating some diurnal inequality (Fig. 2). The estuary was previously investigated by Chanson et al. (2005a); Chanson and Trevethan (2006) and Trevethan et al. (2007a) (Table 1).

The new field E10 study was conducted mid-estuary (Site 2B, Fig. 1) under neap tidal conditions from 6 to 8 June 2007, during which time continuous high frequency turbulence and physio-chemical data were recorded for 50 h. Approximately 44 mm of rain fell in the catchment between 18:00 (5 June 2007) and 09:00 (6 June 2007) when the measurements commenced, while a further 23 mm of rain fell in the first 24 h of data collection (09:00 (6 June 2007) to 09:00 (7 June 2007)). Fig. 2 presents the water depth variations at Site 2B and the measured rainfall as functions of time (in seconds) from 00:00 on 6 June 2007. In Fig. 2, the rainfall data were recorded every 3 h at the Carbrook weather station located approximately 11.5 km from Eprapah Creek estuarine zone, and they were comparable to the daily rainfall data recorded at the Victoria Point sewage treatment plant.

2.2. Instrumentation

For this field investigation, three Sontek™ microADVs and two YSI6600 probes were deployed at Site 2B, approximately 10 m from the left bank. Fig. 1C shows the location of the instruments in the surveyed cross-section. The YSI6600 probes were multi-parameter probes, and the simultaneous measurements included water level, conductivity, temperature, turbidity, pH, dissolved oxygen, and chlorophyll A levels. Table 2 lists the details and location of the instrumentation. In Table 2, each instrument is given a four-symbol code (e.g. ADV1, YSIB) to refer to that instrument.

All the ADV units were synchronised carefully within 20 ms for the entire duration of the study, and the YSI probes were synchronised with the ADVs within a second. All ADV data underwent a thorough post-processing procedure to eliminate any erroneous or corrupted data from the data sets. The post-processing technique was described in Chanson et al. (in press-a, 2005b). Only post-processed data are analysed and discussed herein.

Further details on the field investigation and instrumentation were reported in Trevethan et al. (2007b).

3. Experimental observations

The time-averaged longitudinal velocity data highlighted that the largest ebb and flood velocities occurred around the low tide (Fig. 3). For the ADV1 unit (0.13 m above bed), Fig. 3 shows the time-average and standard deviation of the streamwise velocity V_x together with the water depth as functions of time. V_x is positive downstream, the transverse component V_y is positive towards the left bank, and the vertical velocity component V_z is positive upwards. All the velocity data showed multiple flow reversals around high tides, as well as long-period oscillations. For example, multiple flow reversals are seen in Fig. 3 between $t = 45{,}000$ and 60,000 s, where the time t is counted from 00:00 on 6 June 2007. Similar phenomena were observed previously under neap tide conditions at Eprapah Creek (Chanson, 2003; Trevethan et al., 2006, 2007a). The multiple flow reversals and low-frequency velocity oscillations had periods between 40 min and 1.5 h caused by external resonance linked with some east–west oscillations in the Moreton Bay. Altogether these velocity oscillations were likely to affect the turbulence field in the estuary because the amplitude of the low-frequency velocity oscillations was about that of the tidal current (Fig. 3).

During the field study, the standard deviations of all velocity components varied directly with the magnitude of the longitudinal

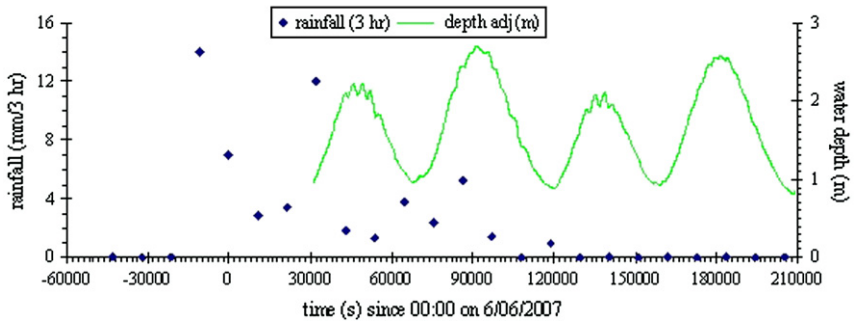

Fig. 2. Measured water depth and rainfall as functions of time at Eprapah Creek on 5, 6, 7 and 8 June 2007 - Time from 00:00 on 6 June 07, water depth recorded at Site 2B by the YSI6600 probe, rainfall data collected every 3 hours at Carbrook weather station.

velocity. They were the largest during the flood tide and during the multiple flow reversals at high tides (Fig. 3). The data illustrated large turbulent velocity fluctuations throughout all the field studies, including during slack tide periods.

The physio-chemical data showed some stratification of the water column for all the study period (Fig. 4). A similar stratification of the water column was observed in two previous studies (E1 and E8) that took place shortly after some intense rainstorms. For the present study, the rainfall was light to moderate and the freshwater runoff discharge was less intense than in the study E8. The water column, however, showed marked differences between the bottom layer and surface waters. Fig. 4 presents the time-variations of water depth, specific conductivity, water temperature and turbidity for both the YSI6600 probes. Air temperature data are reported also in Fig. 4B. The bottom specific conductivity and surface water temperature showed some tidal trend with maximum values around high tides. In contrast, the surface conductivity data showed the presence of a freshwater lens for all the study duration with water conductivities below 10 mS/cm for the entire study. The bottom temperature and surface turbidity were nearly constant for the entire study. The bottom turbidity data showed some marked peaks around two high tide periods ($t = 43{,}000$–$57{,}000$ s and $t = 133{,}000$–$145{,}000$ s) (Fig. 4C). These might be caused by the long-period flow reversals induced by some outer resonance. The pH data also showed marked oscillations at high tide slacks, possibly caused by resonance. Both the dissolved oxygen and chlorophyll A data highlighted some impact of freshwater runoff during first 24 h of the study.

The vertical profiles of physio-chemistry were conducted towards the end of the study on the morning of 8 June 2007. The data showed that the estuarine zone was stratified from 1 km upstream of the river mouth up to the upper estuary, and the freshwater lens was about 1 m thick. A similar vertical stratification was observed during earlier fieldworks with some freshwater runoff (studies E1 and E8). The vertical profiles of physio-chemical parameters suggested that the water column was stratified in terms of specific conductivity, temperature and pH, but it was reasonably well-mixed in terms of dissolved oxygen and turbidity.

3.1. Surface scars and transient fronts

Surface scars were clearly seen at the water surface during the rainfall periods on 6 June 2007. Fig. 5 shows a photographic example taken during the flood tide, but these scars were observed during both flood and ebb tides. The rainfall highlighted some difference in surface roughness; the water surface texture was different in the network of braided "smooth" channels as opposed to the rest of the river. It is acknowledged that such scars are linked with some discontinuity in turbulence characteristics and physio-chemical properties (e.g. Simpson, 1997; Brocchini and Peregrine, 2001; Tamburrino and Gulliver, 2007). The impact of raindrops generated waves and ripples at the water surface and their characteristics were functions of local surface tension. It is conceivable that these channels contained waters of slightly different surface tension compared to the rest of the river. The differences in surface tension might be caused by oils secreted by plants, by emerging groundwater at the riverbed or by substances carried by the water. For example, Wolanski and Ridd (1986) showed that mangrove swamps and flats can trap freshwater volumes which do not mix with the saltwater tidal flux and may remain trapped for a few weeks after the rain event. It is suggested that the surface scars were evidences of longitudinal vortices in the channel, and the analysis of surface photographs indicated that their transverse length scale was between 2 and 3 times the depth. It is also conceivable that the surface scars highlighted some form of density currents.

On 6 June 2007, a few "mini transient fronts" were observed mid-estuary near the end of the flood tide and during the ebb tide. Fig. 6 illustrates such a mini transient front seen at the free surface immediately upstream of Site 2B between 12:20 and 12:30. The mini fronts propagated very slowly upstream. The fronts were barely a ripple at the free surface: i.e., a few millimeters high with

Table 1
Turbulence field measurements at Eprapah Creek Qld, Australia. AMTD: Adopted Middle Thread Distance measured upstream from river mouth

Ref	Dates	Tidal range (m)	ADV system(s)	Sampling rate (Hz)	Sampling duration	Sampling volume
E1	4/04/03	1.84	10 MHz	25	9 × 25 min	AMTD 2.1 km, 14.2 m from left bank, 0.5 m below surface
E2	17/07/03	2.03	10 MHz	25	8 h	AMTD 2.0 km, 7.7 m from left bank, 0.5 m below surface
E3	24/11/03	2.53	10 MHz	25	7 h	AMTD 2.1 km, 10.7 m from left bank, 0.5 m below surface
E4	2/09/04	1.81	10 MHz	25	6 and 3 h	AMTD 2.1 km, 10.7 m from left bank, 0.052 m above bed
E5	8–9/03/05	2.37	10 MHz	25	25 h	AMTD 2.1 km, 10.7 m from left bank, 0.095 m above bed
E6	16–18/05/05	1.36	10 MHz and 16 MHz	25	49 h	AMTD 2.1 km, 10.7 m from left bank, 0.2 and 0.4 m above bed
E7	5–7/06/06	1.58	10 MHz and 16 MHz	25 and 50	50 h	AMTD 3.1 km, 4.2 m from right bank, 0.2 and 0.4 m above bed
E8	28/08/06	2.10	–	–	12 h	AMTD 1.0, 2.1 and 3.1 km
E10	6–8/06/07	1.76	16 MHz	50	50 h	AMTD 2.1 km, 10.7 m from left bank, 0.13 and 0.38 m above bed

Table 2
Details and location of the instruments deployed at Site 2B, Eprapah Creek during field study E10 (6-8 June 2007). f_{scan}: sampling frequency

Instrument Code	Instrument type	Sampling location (m)	f_{scan} (Hz)
ADV1	Sontek 2D-microADV (16 MHz, serial A641F), side-looking head	0.13 m above bed, 10.7 m from left bank	50
ADV2	Sontek 3D-microADV (16 MHz, serial A813F), down-looking head	0.38 m above bed, 10.7 m from left bank	50
ADV3	Sontek 3D-microADV (16 MHz, serial A843F), side-looking head	0.38 m above bed, 10.78 m from left bank	50
YSIB	YSI6600 probe, fixed near bed	0.38 m above bed, 10.4 m from left bank	0.083
YSIF	YSI6600 probe, on float near free surface	0.1 m below surface, 8.3 m from left bank	0.083

wavelength of 2–5 cm, Fig. 6. They were discernable because of the natural light reflection on the free surface (Fig. 6). Visually, the mini front leading edge appeared to be a surface density discontinuity with a plunge point. For the mini transient seen in Fig. 6, the ADV velocity data showed a strong flood velocity ($V_x \sim -0.15$ to -0.25 m/s) while the transverse velocity data V_y exhibited relatively large amplitudes and fluctuations. At the same time, next to the left bank, some fairly strong recirculation was observed in the downstream direction.

3.2. Shear stress

The boundary shear stress was estimated from the velocity gradient next to the bed, although other techniques may be used (see reviews in Schlichting, 1979; Montes, 1998; Koch and Chanson, 2005). The near-bed velocity shear stress was estimated as

$$\tau_o = \rho \times \left(\frac{\kappa \times V_1}{\ln \frac{z_1}{k_s}} \right)^2 \quad (1)$$

where ρ is the fluid density, V_1 is the time-averaged longitudinal velocity of the ADV1 unit located at $z_1 = 0.13$ m, κ is the von Karman constant ($\kappa = 0.4$) and k_s is the equivalent roughness height. Herein the riverbed consisted of gravels and sharp rocks (Fig. 1C) corresponding to $k_s \approx 10$ mm. For the entire field trip, the median shear stress was $\tau_o = 0.0052$ Pa. The boundary shear stress was maximum during the early flood tide and end of the ebb tide when the measured longitudinal velocity amplitude was the largest (Fig. 3).

The boundary shear stress data may be compared with the tangential Reynolds stress $\rho \times \overline{v_x v_z}$ measured at $z_2 = 0.38$ m, as well as with the velocity gradient shear stress, measured between the ADV units 1 and 2, and defined as

$$\tau_{12} = \rho \times \left(\frac{\kappa \times (V_2 - V_1)}{\ln \frac{z_2}{z_1}} \right)^2 \quad (2)$$

For the entire field study, the tangential Reynolds stress and the median velocity gradient shear stress were, respectively, $\rho \times \overline{v_x v_z} = 0.02$ Pa and $\tau_{12} = 0.052$ Pa. For comparison, the median tangential shear stresses $\rho \times \overline{v_x v_y}$ measured by the ADV1 and ADV2 units were 0.024 and 0.031 Pa, respectively.

The findings implied that the turbulent shear in the range $0.13 \text{ m} \le z \le 0.38$ m was one order of magnitude larger than the boundary shear stress (Eq. (1)). The observation differed from turbulence data in a laboratory channel, but a key feature of natural

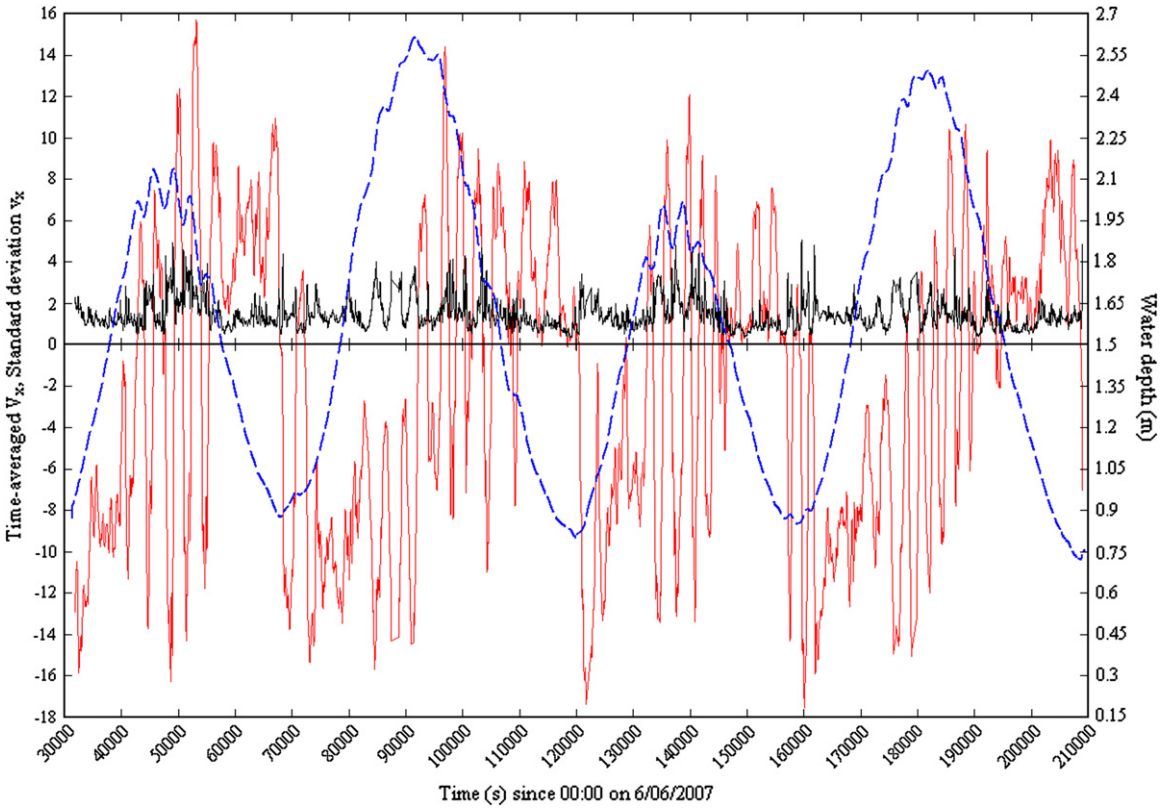

Fig. 3. Time-averaged longitudinal velocity V_x, standard deviation of longitudinal velocity v_x' and water depth as functions of time – data collected by the ADV1 unit, VITA calculations using the average of the next 10,000 samples (200 s) at 10 s intervals along the entire data sets – legend: V_x = solid red line, v_x' = thin black solid line, water depth = thick blue dashed line. For interpretation of the references to colour in this figure legend, the reader is referred to the web version of this article.

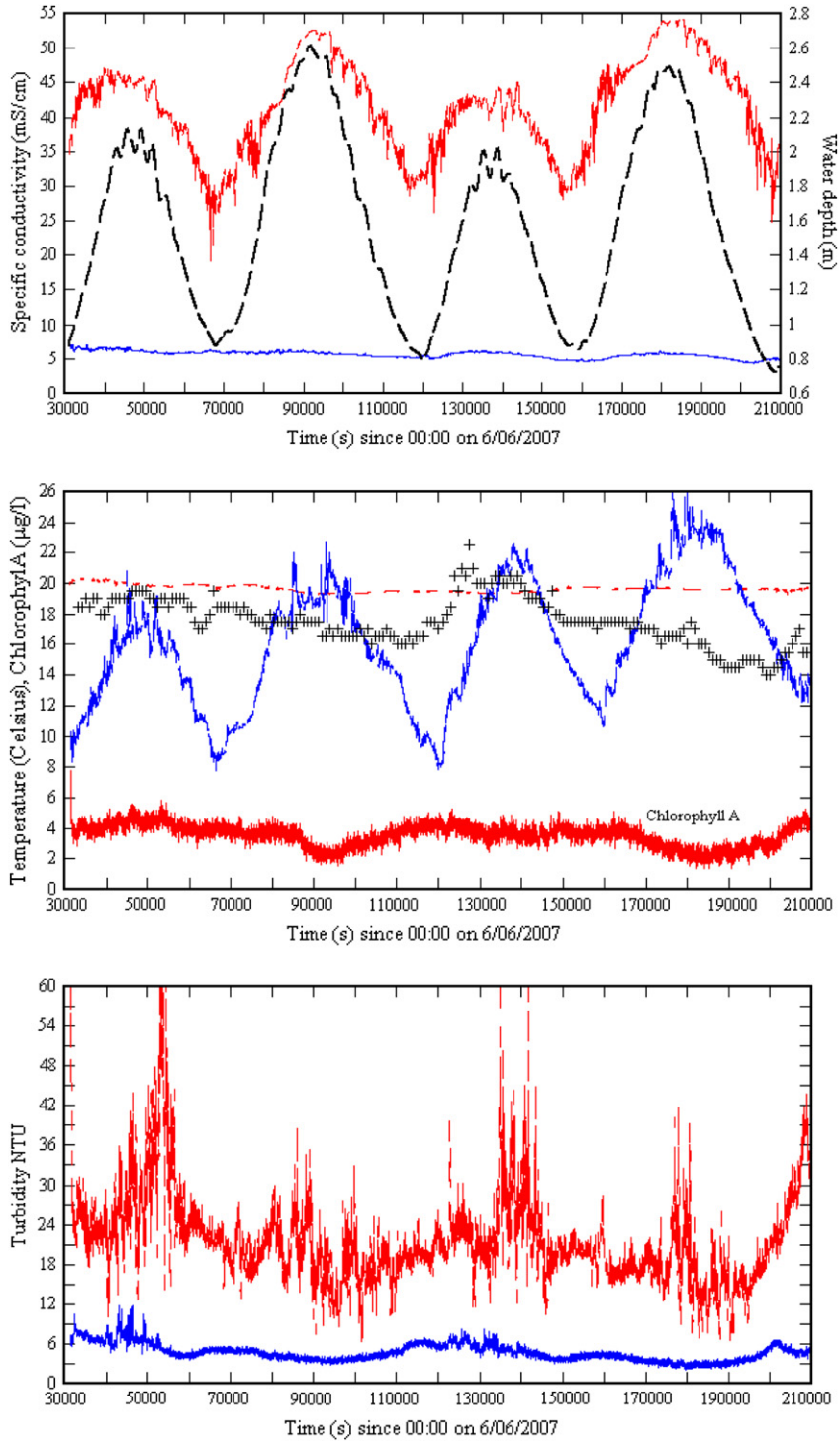

Fig. 4. Water depth, conductivity, temperature and turbidity as functions of time – data collected by the YSI6600 units at Site 2B, Eprapah Creek during the study E10 (6–8 June 2007) – legend: surface probe = solid blue, bottom probe = dashed red, water depth = thick dashed black line. (A) Water depth and specific conductivity. (B) Water and air temperatures (+ = air temperature). (C) Turbidity. For interpretation of the references to colour in this figure legend, the reader is referred to the web version of this article.

estuary flows is the significant three-dimensional effects associated with strong secondary currents.

3.3. Secondary currents

During the field study, some anomalies were observed in terms of the transverse velocity data. The time-averaged transverse velocities $\overline{V_y}$ recorded at $z = 0.13$ and 0.38 m flowed at times in opposite directions for relatively longer durations (e.g. Fig. 7). These anomalies were observed during the flood and ebb tides, and around low tides for the entire study.

These observations suggested the occurrence of some secondary currents associated with strong transverse shear and large tangential stresses $\rho \times \overline{v_x v_y}$ at the sampling location. An example of transverse velocity anomaly is presented in Fig. 7. Fig. 7A shows the instantaneous transverse velocity data V_y together with the

Fig. 5. Surface scars during rainfall periods at Eprapah Creek on 6 June 2007, looking upstream from Site 2B around 09:21 (flood tide).

time-averaged transverse velocity difference during an early flood tide period. Here V_y is positive towards the left bank. Fig. 7A presents about 1 h 23 min of samples, with two large transverse shear events about $t = 160{,}500$ and 163,500 s when the transverse velocities $\overline{V_y}$ recorded at $z = 0.13$ and 0.38 m above the bed flowed in opposite directions: i.e., towards the right and left banks, respectively. The resulting flow pattern is sketched in Fig. 7B showing the vertical profiles of transverse velocity $\overline{V_y}$ and of turbulent velocity v_y' next to the channel bed, where v_y' is the standard deviation of the transverse velocity. The transverse shear pattern sketched in Fig. 7B was further associated with large normal and tangential stresses $\rho \times \overline{v_y v_y}$ and $\rho \times \overline{v_x v_y}$ at both $z = 0.13$ and 0.38 m.

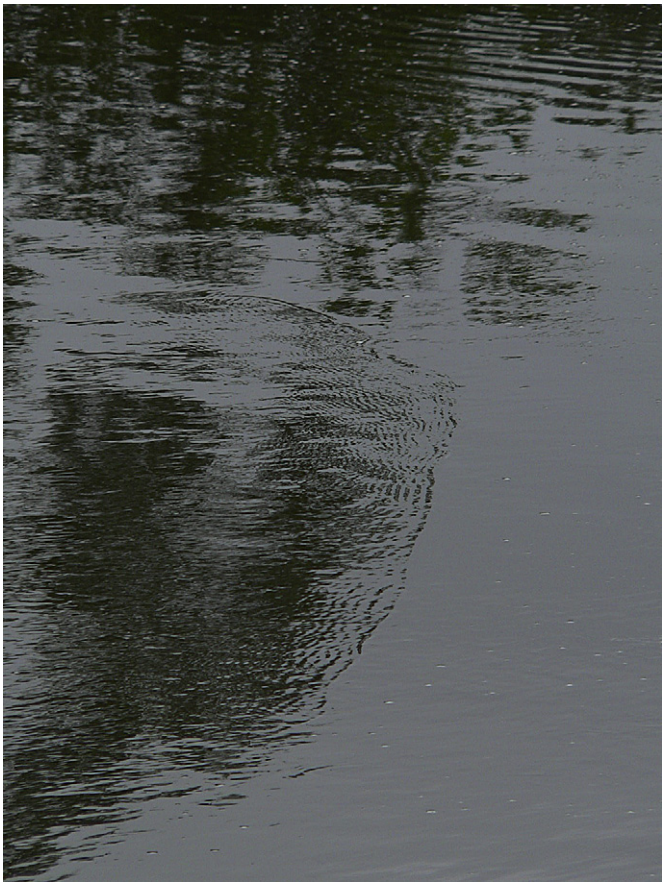

Fig. 6. Mini- transient front observed at Site 2B on 6 June 2007 around 12:29 (end of flood tide), view from the left bank.

More generally, the velocity standard deviation data yielded $v_y'/v_x' \approx 1$ throughout the field study while $v_z'/v_x' \approx 0.62$. The findings were close to recent LES computations in a shallow water channel with similar Reynolds number conditions (Hinterberger et al., 2008). Note that $v_z' < v_x'$ implied some turbulence anisotropy.

Trevethan (2008) discussed the formation of the transverse velocity anomalies in Eprapah Creek, their collapse, and their reformation in the opposite direction. He suggested that the alternance in transverse shear anomalies was linked with the long-period oscillations induced by outer resonance. For example, Fig. 7A illustrates the development of two negative transverse shear events within 50 min. The period is comparable with the long-period oscillation in longitudinal and transverse velocities observed during the present study (e.g. Fig. 3).

4. Covariances and triple correlations of ADV data

The estuary flow exhibited significant spatial variability as evidenced by the simultaneous instantaneous velocity data. Such changes in spatial distribution of the turbulence affected the mixing and transport of suspended sediment and contaminant. Herein, the covariances of the turbulent velocity and acoustic backscatter intensity, and their time-variations throughout the study, are investigated.

4.1. Turbulent velocity

A detailed correlation analysis of the instantaneous velocity data was performed between the three ADV units with the subscripts 1, 2 and 3 referring to the data measured by the ADV1, ADV2 and ADV3 units, respectively (Table 2). Four dimensionless velocity covariances were calculated and Table 3 summarises the median values for the entire study (column 3) and for each 24 h period (columns 4 and 5).

The correlations R_{x1x2}, R_{x2x3} and R_{y1y2} showed some variations with the tides. The covariances R_{x1x2} and R_{x2x3} showed predominantly a positive correlation with the largest values about high tide and smallest about low tide. Periods of negative correlation in terms of R_{x1x2} were likely to result from the relative elevations of the ADV1 and ADV2 units. The ADV1 unit was 0.25 m vertically below the ADV2 unit (Fig. 1C), and such a separation was sufficient to capture flow reversals associated with stratification during the tide changes. The covariance R_{y1y2} was predominantly positive about high tide and predominantly negative about low tide. The changes in the sign of R_{y1y2} were closely linked with the secondary current pattern that was itself a function of the mean flow direction and bathymetry. The covariance R_{y2y3} showed no easily discernable tidal trend although the correlation was predominantly positive during the field study E10. It is worth noting that the velocity covariances R_{x2x3} and R_{y2y3} between ADV2 and ADV3 were larger than the average between $t = 31{,}000$ and 71,000 s (approximately from 09:00 to 20:00 on 6 June 2007). These large covariance values occurred when the majority of rain fell during the study. The trend could possibly be related to the influence of freshwater at Site 2B, and the existence of some discontinuity in turbulence and physio-chemical properties, reflecting perhaps the existence of large streamwise eddies or density currents. The propagation of these coherent structures and the advection of their interfaces past the ADV sampling volumes affected the turbulence characteristics.

Two dimensionless triple correlations were calculated between the three ADV units. That is, R_{x1x2x3} and R_{y1y2y3}, where $R_{x1x2x3} = \overline{v_{x1} v_{x2} v_{x3}}/v'_{x1} v'_{x2} v'_{x3}$, for example. Overall, the fluctuations of the triple correlations seemed the largest about the ebb tide and smallest about the flood tide. Large fluctuations in both the triple

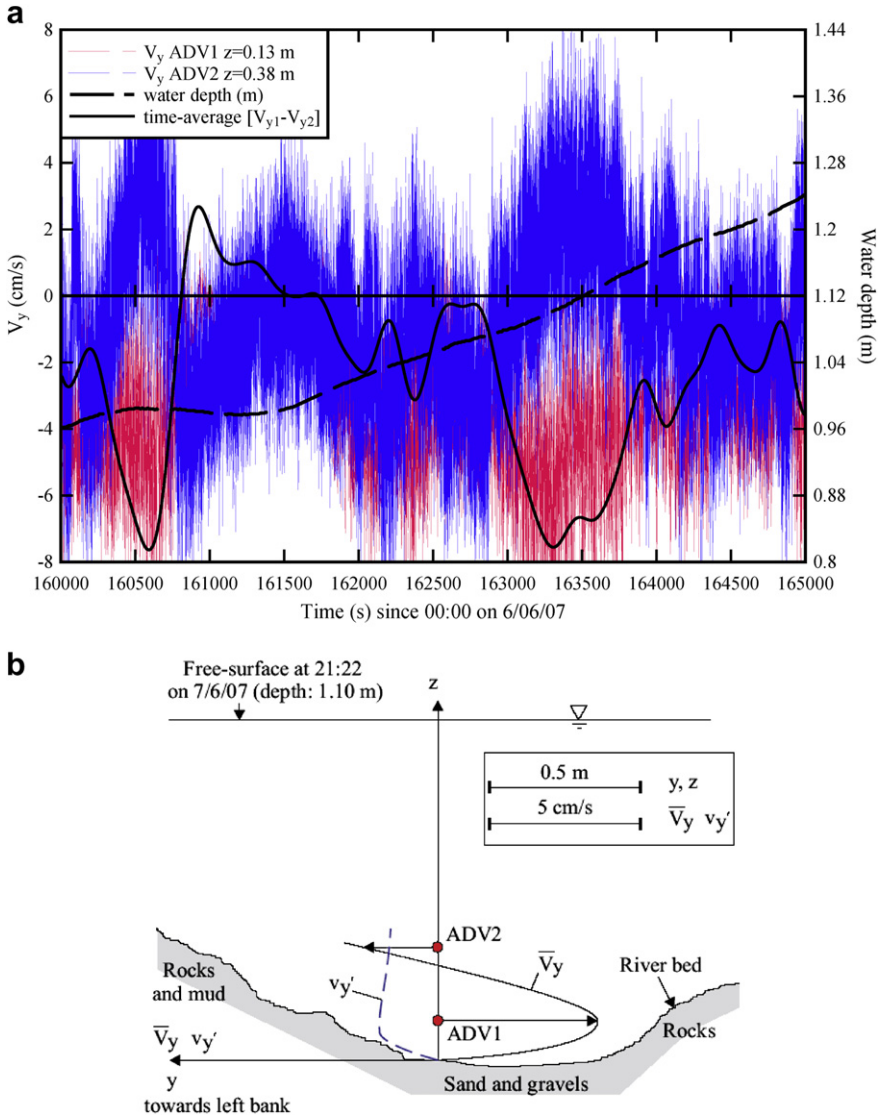

Fig. 7. Transverse shear flow pattern at the sampling site. (A) Instantaneous transverse velocities V_y for the ADV1 ($z_1 = 0.13$ m) and ADV2 ($z_2 = 0.38$ m) units and time-averaged transverse velocity gradient ($V_{y1} - V_{y2}$) during an early flood tide (7 June 2007 evening). (B) Dimensioned sketch of the vertical profiles of transverse velocity $\overline{V_y}$ and turbulent velocity v_y' at the sampling site for $t = 163{,}300$ s (21:22 on 7 June 2007) (looking downstream).

correlations were possibly associated with the long-period oscillations in terms of the longitudinal velocity V_x. Greater flow depths with corresponding changes to the stratification profile might lead to negatively correlated fluctuations which resulted in lesser fluctuations of triple correlations during high water periods, and greater fluctuations of R_{x1x2x3} and R_{y1y2y3} during the early ebb tide. Table 3 shows that the absolute value of the covariance R_{x2x3} was generally higher than that of R_{x1x2}. Hence, the triple correlation R_{x1x2x3} received a significant contribution from R_{x2x3}, and this was consistent with the lower spatial proximity between the ADV2 and ADV3 units than between the ADV1 and ADV2 units.

4.2. ADV backscatter intensity

The acoustic backscatter intensity signal of each ADV unit was analysed. The backscatter intensity is a function of the ADV signal amplitude that is proportional to the number of particles within the sampling volume:

$$I_b = 10^{-5} 10^{0.043\mathrm{Ampl}} \quad (3)$$

where the average amplitude Ampl is in counts. The backscatter intensity I_b may be used as a proxy for the instantaneously suspended sediment concentration (SSC) because of the strong relationship between I_b and SSC (Thorne et al., 1991; Fugate and Friedrichs, 2002; Chanson et al., in press-b). The present field data showed large fluctuations in backscatter intensity during the entire field study. The median values of the dimensionless fluctuations $I_b'/\overline{I_b}$ were 0.54, 0.46 and 0.46 for the ADV1, ADV2 and ADV3 units, respectively. The large fluctuation magnitudes were consistent with earlier results at Eprapah Creek (Chanson et al., 2007; Trevethan et al., 2007a). The results also showed larger fluctuation levels at low tides when the turbulent Reynolds stresses were the largest.

The dimensionless covariances of ADV backscatter intensity were calculated: i.e., R_{b1b2}, R_{b2b3} and R_{b1b3} where $R_{b1b2} = \overline{I_{b1} I_{b2}}/I_{b1}' I_{b2}'$, for example. Fig. 8 shows the time-variations of the dimensionless covariance R_{b2b3}. Overall the covariance data tended to vary with the tides, with the correlations increasing slightly about the high tides, although the covariance magnitudes were relatively small ($R < 0.3$) and predominantly positive.

Table 3
Median values of dimensionless covariances and triple-correlations

Parameter	Definition	Entire study	$t = 30{,}000$–$120{,}000$ s	$t = 120{,}000$–$210{,}000$ s
(1)	(2)	(3)	(4)	(5)
R_{x1x2}	$\overline{v_{x1}v_{x2}}/v'_{x1}v'_{x2}$	0.255	0.254	0.256
R_{x2x3}	$\overline{v_{x2}v_{x3}}/v'_{x2}v'_{x3}$	0.427	0.470	0.382
R_{y1y2}	$\overline{v_{y1}v_{y2}}/v'_{y1}v'_{y2}$	−0.0109	−0.0083	−0.0135
R_{y2y3}	$\overline{v_{y2}v_{y3}}/v'_{y2}v'_{y3}$	0.299	0.437	0.232
R_{x1x2x3}	$\overline{v_{x1}v_{x2}v_{x2}}/v'_{x1}v'_{x2}v'_{x3}$	−0.0051	−0.0048	−0.0054
R_{y1y2y3}	$\overline{v_{y1}v_{y2}v_{y2}}/v'_{y1}v'_{y2}v'_{y3}$	0	−0.0032	0.00345
R_{b1b2}	$\overline{I_{b1}I_{b2}}/I'_{b1}I'_{b2}$	0.0074	0.0089	0.0062
R_{b2b3}	$\overline{I_{b2}I_{b3}}/I'_{b2}I'_{b3}$	0.0175	0.023	0.0132
R_{qx1qx2}	$\overline{I_{b1}V_{x1}I_{b2}V_{x2}}/(I_{b1}V_{x1})'(I_{b2}V_{x2})'$	0.0342	0.0315	0.037
R_{qx2x3}	$\overline{I_{b2}V_{x2}I_{b3}V_{x3}}/(I_{b2}V_{x2})'(I_{b3}V_{x3})'$	−0.0033	−0.0018	−0.0049
R_{qy1qy2}	$\overline{I_{b1}V_{y1}I_{b2}V_{y2}}/(I_{b1}V_{y1})'(I_{b2}V_{y2})'$	0.0605	0.0693	0.0519
R_{qy2qy3}	$\overline{I_{b2}V_{y2}I_{b3}V_{y3}}/(I_{b2}V_{y2})'(I_{b3}V_{y3})'$	0.168	0.238	0.125

However, the largest covariance values of R_{b1b2}, R_{b2b3} and R_{b1b3} seemed to occur between $t = 40{,}000$ and 60,000 s, during which an increase in all covariances of backscatter intensity was observed (Fig. 8). Since the spatial separation of the ADV2 and ADV3 units was 0.08 m (Fig. 1C), it may be inferred that the scalar length scale of the flow at this point was generally less than 0.08 m, but there were periods during which the scalar length scale exceeded this value.

Defining the pseudo-longitudinal and transverse suspended sediment fluxes $q_{x1} = I_{B1}V_{x1}$ and $q_{y1} = I_{B1}V_{y1}$ for ADV1 unit, the dimensionless covariances of pseudo streamwise and transverse suspended sediment flux were calculated (Table 3). Fig. 9 shows the time-variations of the dimensionless covariances R_{qx2qx3} and R_{qy2qy3}. Overall the correlations R_{qx1qx2}, R_{qx2qx3} and R_{qy1qy2} seemed to vary with the tides, but R_{qy2qy3} showed no easily discernable tidal pattern. The covariances R_{qx1qx2} and R_{qx2qx3} were predominantly positive throughout the investigation period and seemed the largest about high tides and lowest about low tides (Fig. 9A). The covariance R_{qy1qy2} showed some predominantly positive values about high tide and predominantly negative values about low tide. Note the large covariance values of R_{qy2qy3} between $t = 31{,}000$ and 71,000 s (approximately from 09:00 to 20:00 on 6 June 2007). The increased covariance levels were observed when the majority of the rain fell for the study E10, and could be conceivably related to the influence of freshwater runoff.

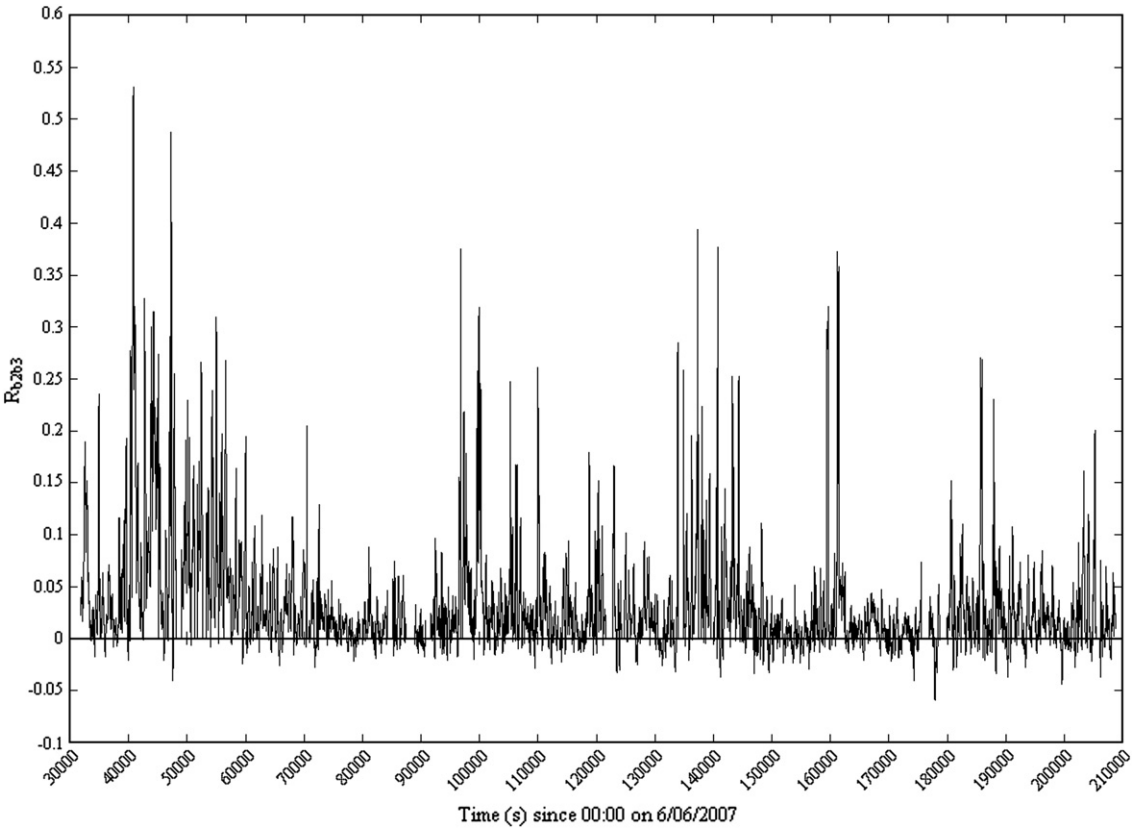

Fig. 8. Dimensionless ADV backscatter intensity covariance R_{b2b3} as a function of time – data collected at Site 2B, Eprapah Creek during the study E10 (6–8 June 2007) – calculations conducted over 10,000 data points (200 s) every 10 s along entire data sets.

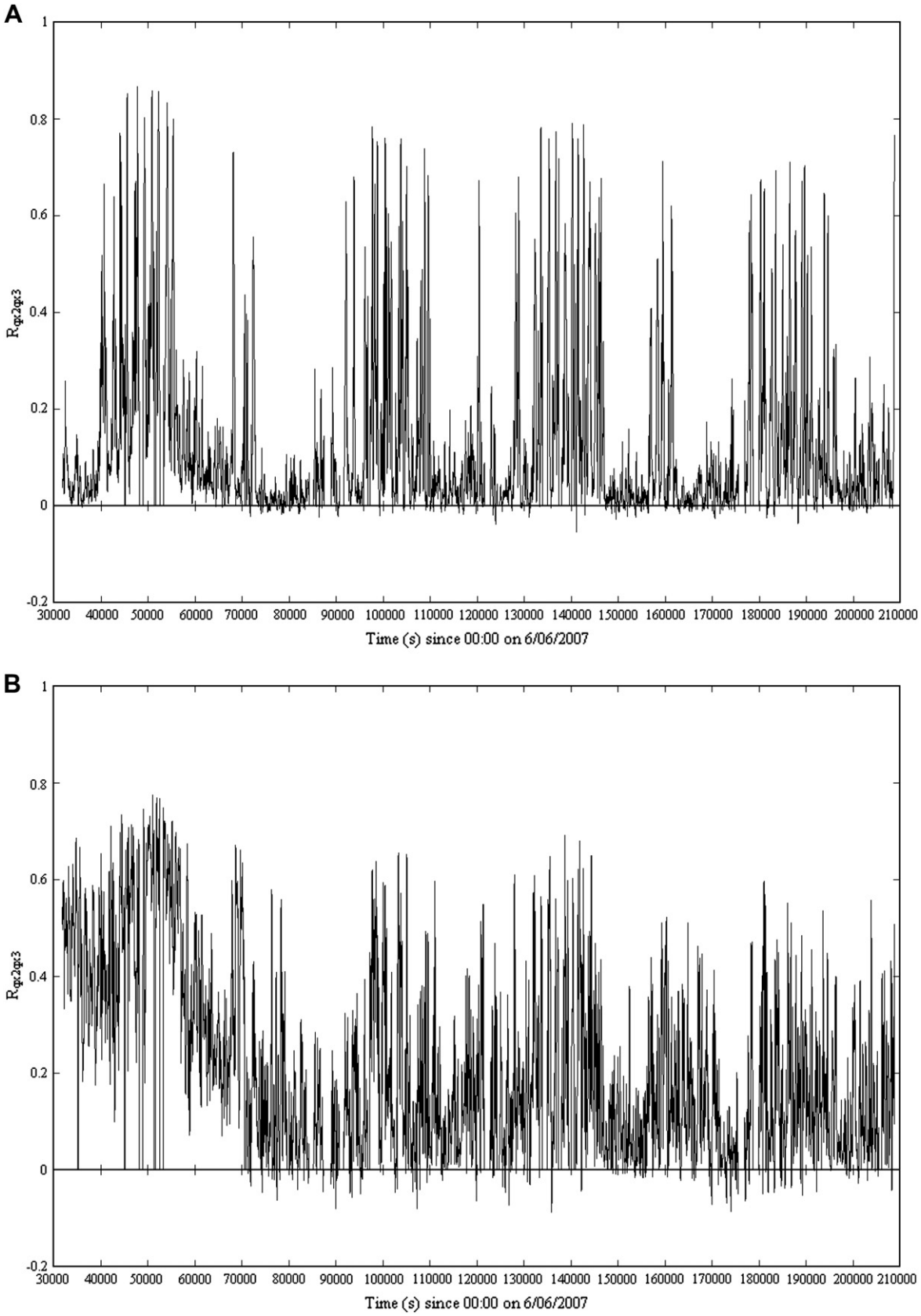

Fig. 9. Dimensionless pseudo-sediment flux covariances R_{qx2qx3} and R_{qy2qy3} as functions of time – data collected at Site 2B, Eprapah Creek during the study E10 (6–8 June 2007) – calculations conducted over 10,000 data points (200 s) every 10 s along entire data sets. (A) R_{qx2x3}. (B) R_{qy2qy3}.

5. Conclusion

In natural estuaries, the suspended sediment processes are driven by the turbulent momentum mixing. Detailed turbulence field measurements were conducted in a small subtropical estuary with semi-diurnal tides under neap tide conditions. Three acoustic Doppler velocimeters were installed in the middle estuarine zone at fixed locations, and were sampled simultaneously and continuously at relatively high frequency (50 Hz) for 50 h.

The results illustrated the influence of tidal forcing for this type of small estuary. Some turbulent properties were similar to classical turbulent boundary layer results (e.g. vertical turbulence ratio v_z'/v_x'), but others differed from classical boundary layer properties, including the horizontal turbulence intensity v_y'/v_x'. Low-frequency longitudinal velocity oscillations and multiple flow reversals at high waters were observed and believed to be induced by external resonance in Moreton Bay. The physio-chemical data showed some stratification of the water column for the whole study period. The boundary shear stress data implied that the turbulent shear in the range 0.13 m $\leq z \leq$ 0.38 m was one order of magnitude larger than the boundary shear. This observation differed from turbulence data in a laboratory channel, but a key feature of the natural estuary flow was the significant three-dimensional effects associated with strong secondary currents. Indeed, some anomalies were observed in terms of the transverse velocity data during the study.

The velocity covariances and triple correlations, and their variations with time, were investigated. Similarly, the backscatter intensity and pseudo-sediment flux covariances were estimated. The covariances of the longitudinal velocity components showed some tidal trend, and the covariances of the transverse horizontal velocity component exhibited trends that reflected changes in secondary current patterns between ebb and flood tides. These secondary currents were caused by the three-dimensional nature of the flow in this natural system. The acoustic backscatter intensity data were characterised by large fluctuations during the entire study, with the dimensionless fluctuation intensity $I_b'/\overline{I_b}$ between 0.46 and 0.54, implying large fluctuations in suspended sediment concentration and mass fluxes. The covariances of backscatter intensity showed little tidal trend although larger covariance values were observed at high tide.

An unusual aspect of the field study was some moderate rainfall prior to and during the first part of the sampling period. Visual observations highlighted some surface scars and marked channels, while some mini transient fronts were observed. Overall the rainfall was moderate and it had relatively little impact on the estuarine turbulence compared to intense rainstorm events.

Acknowledgements

The writers thank John Ferris (Qld EPA) for his contributions during the fieldwork, as well as all fieldwork participants. Hubert Chanson thanks Dr. Eric Jones and Dr. Eric Wolanski for their advice.

References

Bowden, K.F., Ferguson, S.R., 1980. Variations with height of the turbulence in a tidally-induced bottom boundary layer. In: Nihoul, J.C.J. (Ed.), Marine Turbulence. Elsevier, Amsterdam, The Netherlands, pp. 259–286.

Brocchini, M., Peregrine, D.H., 2001. The dynamics of strong turbulence at free surfaces. Part 1. Description. Journal of Fluid Mechanics 449, 225–254.

Chanson, H., 2003. A hydraulic, environmental and ecological assessment of a subtropical stream in eastern Australia: Eprapah Creek, Victoria Point QLD on 4 April 2003. Report No. CH52/03, Department of Civil Engineering, The University of Queensland, Brisbane, Australia, June, 189 p.

Chanson, H., Brown, R., Ferris, J., Ramsay, I., Warburton, K., 2005a. Preliminary measurements of turbulence and environmental parameters in a sub-tropical estuary of eastern Australia. Environmental Fluid Mechanics 5 (6), 553–575, doi:10.1007/s10652-005-0928-y.

Chanson, H., Trevethan, M., 2006. Turbulence in small sub-tropical estuary with semi-diurnal tides. In: Proceedings of Second International Conference on Estuaries and Coasts (ICEC-2006), Guangzhou, Guangdong Province, China, 28–30 November, Invited Paper, vol. I. Guangdong Economy Publications, pp. 140–151.

Chanson, H., Trevethan, M., Aoki, S., 2005b. Acoustic Doppler Velocimetry (ADV) in a small estuarine system. Field experience and "Despiking". In: Jun, B.H., Lee, S.I., Seo, I.W., Choi, G.W. (Eds.), Proceedings of the 31st Biennial IAHR Congress, Seoul, Korea, pp. 3954–3966. Theme E2, Paper 0161.

Chanson, H., Takeuchi, M., Trevethan, M., 2007. High-frequency suspended sediment flux measurements in a small estuary. In: Sommerfield, M. (Ed.), Proceedings of the Sixth International Conference on Multiphase Flow ICMF 2007, Leipzig, Germany, 9–13 July, Session 7, Paper No. S7_Mon_C_S7_Mon_C_5, 12 p. (CD-ROM).

Chanson, H., Trevethan, M., Aoki, S., in press-a. Acoustic Doppler Velocimetry (ADV) in small estuary: field experience and signal post-processing. Flow Measurement and Instrumentation 19, DOI: 10.1016/j.flowmeasinst.2008.03.003.

Chanson, H., Takeuchi, M., Trevethan, M., in press-b. Using turbidity and acoustic backscatter intensity as surrogate measures of suspended sediment concentration in a small sub-tropical estuary. Journal of Environmental Management 86 (4), DOI: 10.1016/j.jenvman.2007.07.009.

Digby, M.J., Saenger, P., Whelan, M.B., McConchie, D., Eyre, B., Holmes, N., and Bucher, D., 1999. A physical classification of Australian estuaries. Report No. 9, LWRRDC, Australia, National River Health Program, Urban Sub-program, Occasional Paper, 16/99.

Fugate, D.C., Friedrichs, C.T., 2002. Determining concentration and fall velocity of estuarine particle populations using ADV, OBS and LISST. Continental Shelf Research 22, 1867–1886.

van de Ham, T., Fromtijn, H.L., Kranenburg, C., Winterwerp, J.C., 2001. Turbulent exchange of fine sediments in a tidal channel in the Ems/Dollard estuary. Part I: turbulence measurements. Continental Shelf Research 21, 1605–1628.

Hinterberger, C., Fröhlich, J., Rodi, W., 2008. 2D and 3D turbulent fluctuations in open channel flow with $Re_\tau = 590$ studied by large eddy simulation. Flow, Turbulence, Combustion 80 (2), 225–253, doi:10.1007/s10494-007-9122-2.

Kawanisi, K., 2004. Structure of turbulent flow in a shallow tidal estuary. ASCE. Journal of Hydraulic Engineering 130 (4), 360–370.

Kawanisi, K., Yokosi, S., 1994. Mean and turbulence characteristics in a tidal river. Continental Shelf Research 17 (8), 859–875.

Koch, C., Chanson, H., 2005. An experimental study of tidal bores and positive surges: hydrodynamics and turbulence of the bore front. Report No. CH56/05, Department of Civil Engineering, The University of Queensland, Brisbane, Australia, July, 170 p.

Montes, J.S., 1998. Hydraulics of Open Channel Flow. ASCE Press, New York, USA, 697 p.

Nikora, V., Goring, D., Ross, A., 2002. The structure and dynamics of the thin near-bed layer in a complex marine environment: a case study in Beatrix Bay, New Zealand. Estuarine, Coastal and Shelf Science 54, 915–926.

Ralston, D.K., Stacey, M.T., 2005. Stratification and turbulence in subtidal channels through intertidal mudflats. Journal of Geophysical Research, AGU, 110, Paper C08009, 16 p.

Schlichting, H., 1979. Boundary Layer Theory, seventh ed. McGraw-Hill, New York, USA.

Shiono, K., West, J.R., 1987. Turbulent perturbations of velocity in the Conwy estuary. Estuarine, Coastal and Shelf Science 25, 533–553.

Simpson, J.E., 1997. Gravity Current in the Environment and the Laboratory, second ed. Cambridge University Press, Cambridge, UK, 244 p.

Stacey, M.T., Monismith, S.G., Burau, J.R., 1999. Observations of turbulence in a partially stratified estuary. Journal of Physical Oceanography 29, 1950–1970.

Tamburrino, A., Gulliver, J.S., 2007. Free-surface visualization of streamwise vortices in a channel flow. Water Resources Research 43, doi:10.1029/2007WR005988, Paper W11410, 12 p.

Thorne, P.D., Vincent, C.E., Hardcastle, P.J., Rehman, S., Pearson, N., 1991. Measuring suspended sediment concentrations using backscatter devices. Marine Geology 98, 7–16.

Trevethan, M., 2008. A fundamental study of turbulence and turbulent mixing in a small subtropical estuary. Ph.D. thesis, Department of Civil Engineering, The University of Queensland, 342 p.

Trevethan, M., Chanson, H., Brown, R.J., 2006. Two series of detailed turbulence measurements in a small subtropical estuarine system. Report No. CH58/06, Division of Civil Engineering, The University of Queensland, Brisbane, Australia, March, 153 p.

Trevethan, M., Chanson, H., Takeuchi, M., 2007a. Continuous high-frequency turbulence and sediment concentration measurements in an upper estuary. Estuarine, Coastal and Shelf Science 73 (1–2), 341–350, doi:10.1016/j.ecss.2007.01.014.

Trevethan, M., Chanson, H., Brown, R.J., 2007b. Turbulence and turbulent flux events in a small subtropical estuary. Report No. CH65/07, Hydraulic Model Report Series, Division of Civil Engineering, The University of Queensland, Brisbane, Australia, November, 67 p.

Voulgaris, G., Meyers, S.T., 2004. Temporal variability of hydrodynamics, sediment concentration and sediment settling in a Tidal Creek. Continental Shelf Research 24, 1659–1683.

Wolanski, R., Ridd, P., 1986. Tidal mixing and trapping in mangrove swamps. Estuarine, Coastal and Shelf Science 23, 759–771.